THE JOURNAL OF PHYSICAL CHEMISTRY B

ARTICLE

pubs.acs.org/JPCB

Temperature-Induced Transition from Odd−Even to Even−Odd Effect in Polyelectrolyte Multilayers Due to Interpolyelectrolyte Interactions

Peter Nestler,[†] Stephan Block,[*,†,‡] and Christiane A. Helm[*,†]

[†]Institut für Physik, Ernst-Moritz-Arndt Universität, Felix-Hausdorff-Str. 6, D-17487 Greifswald, Germany

[‡]ZIK HIKE—Zentrum für Innovationskompetenz "Humorale Immunreaktionen bei kardiovaskulären Erkrankungen", Fleischmannstr. 42−44, D-17475 Greifswald, Germany

Supporting Information

ABSTRACT: Within a liquid cell the linear growth of polyelectrolyte multilayers from poly(styrenesulfonate) (PSS) and poly(allylamine hydrochloride) (PAH) is observed with multiple angle null ellipsometry. The salt content is varied between 1 and 4 mol/L NaCl and the temperature between 20 and 55 °C. In the linear growth regime, the outermost layer is investigated. At low temperature, a top PSS layer is twice as thick as a top PAH layer (odd−even effect), consistent with the respective monomer volumes and the same water content for both kinds of top polyelectrolyte layers as confirmed by refractive index measurements. On heating, the thickness of a polycation/polyanion bilayer increases. For temperatures exceeding a crossover temperature, a top PAH layer is thicker than a top PSS layer (even−odd effect). Simultaneously, the index of refraction of the respective top layers indicates a compact PSS and a swollen PAH layer. It is suggested that, at elevated temperature and high salt conditions, secondary forces gain importance in comparison to electrostatic forces: therefore, a transition from an odd−even to an even−odd effect occurs, as well as the decreased film stability on drying as described before (Cornelsen, M., et al. Macromolecules 2010, 43, 4300). The ellipsometric data indicate that PAH/PSS layer pairs exceeding 8.6 nm thickness in solution are unstable in air.

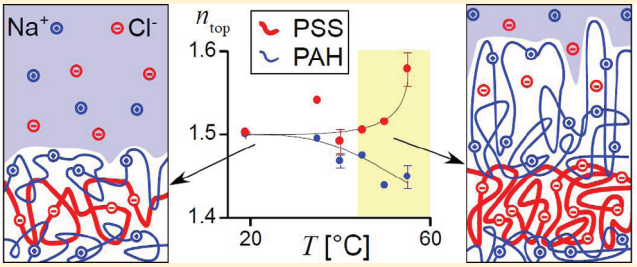

INTRODUCTION

Adsorbed polyelectrolytes (PEs) are used in a multitude of technical applications (e.g., as wet and dry strength additives), but also in basic research in connection with material and the life sciences.[2−6] Due to their ionizable groups (incorporated within the monomeric units), polyelectrolytes can be used as flocculating or dispersing agent in industrial applications.[7,8] Additionally, by sequential adsorption of oppositely charged polyelectrolytes onto surfaces, it is possible to build polyelectrolyte multilayers (PEMs) onto planar as well as curved solid substrates.[2,9] Interestingly, several multilayer properties can be adjusted, which enables to create self-assembling smart interfaces.[10,11] Moreover, as macromolecules like proteins can be incorporated into the layer, hollow capsules made of PEMs are also considered as key strategy in targeted drug delivery.[12]

Various PEM properties can be controlled during the adsorption process. For example, the thickness can be influenced by the number of adsorption steps, the polyelectrolytes used, and the properties of the adsorption solution (like ionic strength c_{salt}, temperature T, and pH value). Hence, a control of the layer thickness with nanometer precision is possible,[13] if the dependence of the PEM growth on the preparation conditions is known. Therefore, enormous experimental work has been done to understand the processes involved in sequential adsorption of polyelectrolyte layers.[14]

Recently, it was found that certain PEMs exhibit a pronounced temperature effect, which is characterized by a strong increase in average thickness per polycation−polyanion bilayer if a certain transition temperature T_{trans} is exceeded.[15] For example, for PEMs made of poly(styrenesulfonate) (PSS) and poly(allylamine hydrochloride) (PAH), it was shown (i) that this transition temperature T_{trans} decreases with the salt concentration c_{salt} in the deposition solution and (ii) that PEMs built below and above T_{trans} differ noticeably in terms of water content, roughness, and layer stability.[1,16] Taking these findings together, it was argued that nonelectrostatic effects might play a big role in the temperature effect of PEMs.[16] All these are interesting, yet qualitative observations and a consistent picture are still lacking.

To understand the interplay of electrostatic and nonelectrostatic forces (especially of hydrophobic nature) it would be beneficial to investigate the dependence of the salt concentration and deposition temperature on the layer structure. A systematic variation of these properties would allow studying competitive interactions which influence the formation of polyelectrolyte multilayers on a fundamental level. Unfortunately, such investigations are obscured by the fact that the necessary preparation

Received: September 13, 2011
Revised: December 19, 2011
Published: December 28, 2011

conditions (high salt concentration and deposition temperature) often lead to a pronounced layer destabilization that occurs during the drying of the PEM. This destabilization is characterized by a drastic increase in layer roughness and frequently, even a detachment or partial dewetting of the PEM is observed.[1] Hence, the investigation of the temperature effect requires in situ techniques like ellipsometry, neutron, or optical reflectometry, which are capable of exploring PEMs in its liquid environement.

In previous ellipsometric studies,[17,18] it was observed that a deposition of about 8−12 layers is necessary to achieve linear multilayer growth (see Figure 3). The differences in growth of the first layers (adjacent to the substrate) and the bulk PEM are often interpreted in terms of a zone model: it states that the conformation of polyelectrolytes is disturbed in the vicinity of the substrate (due to the spatial confinement), leading to less dense and more hydrated layers. After the deposition of a certain amount of PE layers, the influence of the substrate becomes negligible, which allows the linear layer growth of the bulk PAH/PSS-PEM.[17,18]

Moreover, ellipsometry and other in situ techniques showed that even in the linear-growth regime (>12 layers) it is also important if the PEM consists of an odd or an even number of polyelectrolyte layers as various properties might depend on the terminating layer. Since polyanion-terminated films consist of an odd number of layers and polycation-terminated layers of an even number, these effects are termed "odd−even" effects.[19] In the past years, such effects have been observed for many PEM properties like water immobilization, swelling/drying behavior, and electrophoretic mobility.[20−22] Interestingly, it is often supposed that the whole PEM layer contributes to these odd−even effects, which means that the investigated property alternates during the deposition steps in the whole PEM volume. For example, using NMR, Schönhoff and co-workers show that the occurrence of odd−even variations in water immobilization depends on the composition of the PEM (for PAH/PSS an odd−even effect is observed, but not for PDADMAC/PSS).[21] Interestingly, by solely changing the composition of the last layer, they successfully proved that the alternating behavior itself depends only on the charge of the outmost polyelectrolyte layer, but not directly on its chemical composition. Hence, the ability of the PEM to show alternation depends on the composition of most of the PEM, while the alternation itself is ruled in this case only by the outmost layer. These and similar observations led to the conclusion that odd−even effects are volume effects.[21]

To shed light on this question, we investigate the PEM built up using a null ellipsometer which is able (i) to measure at a solid−liquid interface and (ii) to determine the ellipsometric angles at various angles of incidence (multiple angle ellipsometer). The setup allows to resolve PEM thickness and index of refraction (i) directly during the deposition (the sample is prepared and measured inside the ellipsometer; movement into a measurement device or layer modification like drying is not necessary) and (ii) with high precision (as the measurement of the ellipsometric angles over an interval instead of a single fixed angle of incidence generally yields a much higher content of information).

Using this approach, we reproduce the finding that a PSS layer is twice as thick as a PAH layer if the PEM is deposited at room temperature, which leads to an odd−even variation of the PEM thickness increment (with respect to the deposition steps). Surprisingly, at high salt concentration and deposition temperature, this variation inverses into an even−odd one. Moreover, we observe a similar alternation in the PEM index of refraction, which allows us to determine the water content of the outmost layer. We use this special property of PAH/PSS-PEMs to show that both polyelectrolytes differ strongly in their level of hydration and chain conformation after physisorption and that the particular layers contribute to a different extent to the temperature effect.

MATERIALS

Poly(styrenesulfonate) sodium salt (PSS; M_w = 340 kDa and PDI < 1.1) was obtained from Polymer Standard Service (Mainz, Germany); poly(allylamine hydrochloride) (PAH; M_w = 56 kDa) and branched poly(ethylenime) (PEI; M_w = 75 kDa) were purchased from Sigma-Aldrich (Steinheim, Germany). Sodium chloride (NaCl; pro analysis grade) was obtained from Merck (Darmstadt, Germany). All solutions were prepared with ultrapure water using a Milli-Q device (Millipore, Billerica, MA).

Polished silica (100) wafers (Wacker Siltronic AG, Burghausen, Germany) were used as substrates. The wafers were cleaned according to the RCA standard and used fresh.

Each polyelectrolyte (PE) deposition solution contains a concentration of 3 mM of the respective PE (with respect to the monomer concentration). The substrate is functionalized by the adsorption of one PEI layer dissolved in pure water (21 °C). The salt concentrations of the PSS and PAH deposition solutions are set to a value of either 1, 2, 3, or 4 M by dissolving the corresponding amount of NaCl within the PE solutions. For each set of PE solutions, a washing solution (having the same NaCl concentration as the deposition solution) is used.

ELLIPSOMETRY

PEM film thicknesses and indices of refraction are measured with ellipsometry. The measurements are performed with a null ellipsometer (Multiskop; Optrel GbR, Kleinmachnow, Germany) in PCSA configuration (polarizer−compensator−sample−analyzer). A He−Ne laser (power = 4 mW; wavelength λ = 632.8 nm) is used as light source. The measured quantities are the ellispometric angles Ψ and Δ, which correspond to the changes in amplitude and phase of the light due to reflection at the sample.

With this ellipsometer, the angles Ψ and Δ are calculated from the positions of polarizer P and analyzer A, which lead to light extinction. This is generally achieved (for a fixed compensator) for two different pairs of (P, A), which are called different ellipsometric zones.[23]

The ellipsometric angles are related to the ratio of the Fresnel reflection coefficients by

$$\frac{r_p}{r_s} = \tan(\Psi)\exp(i\Delta) \quad (1)$$

where r_p and r_s are the reflection coefficients of the parallel and normal components of the electric vector E (with respect to the plane of incidence).

For further analysis the ellipsometric angles were numerically simulated by a slab model of the sample (cf. Figure 1): the structure of the layer perpendicular to the surface is represented by a stack of four slabs, each with a constant refractive index (Si substrate, SiO_2 layer, PEM, and surrounding solution). The roughnesses between different slabs are set to zero.

The laser light is reflected at each interface where the refractive index changes. For the three interfaces Si−SiO_2, SiO_2−PEM,

and PEM−solution, the reflection coefficients $r_k(\mathrm{Si-SiO_2})$, $r_k(\mathrm{SiO_2-PEM})$, and $r_k(\mathrm{PEM-solution})$ are calculated according to the Fresnel equations (index k represents the p- and the s-components, respectively). These reflection coefficients are solely determined by the angle of incidence and the refractive indices of the materials.

To obtain the reflectance of the SiO_2 layer, the contributions of the interfaces substrate/SiO_2 and SiO_2/PEM have to be summed up, which leads (in the case of homogeneous slabs) to

$$r_k(\mathrm{SiO_2}) = \frac{r_k(\mathrm{Si-SiO_2}) + r_k(\mathrm{SiO_2-PEM})e^{i\delta\varphi(\mathrm{SiO_2})}}{1 + r_k(\mathrm{Si-SiO_2})r_k(\mathrm{SiO_2-PEM})e^{i\delta\varphi(\mathrm{SiO_2})}} \quad (2)$$

The reflectivity of the multilayered system (cf. Figure 1) is then calculated by recursion

$$r_k(\mathrm{PEM}) = \frac{r_k(\mathrm{SiO_2}) + r_k(\mathrm{PEM-solution})e^{i\delta\varphi(\mathrm{PEM})}}{1 + r_k(\mathrm{SiO_2})r_k(\mathrm{PEM-solution})e^{i\delta\varphi(\mathrm{PEM})}} \quad (3)$$

$\delta\varphi(\mathrm{SiO_2})$ and $\delta\varphi(\mathrm{PEM})$ denote the phase shifts of the respective slabs.[24] Note that $\delta\varphi(\mathrm{PEM})$ is the only parameter which depends on the thickness of the PEM according to $\delta\varphi(\mathrm{PEM}) = 2\pi d_{\mathrm{PEM}} n_{\mathrm{PEM}}/\lambda$ (d_{PEM} denotes PEM film thickness and n_{PEM} the PEM refractive index). Therefore, the ellipsometric angles are given by

$$\frac{r_p(\mathrm{PEM})}{r_s(\mathrm{PEM})} = \tan(\Psi)\exp(i\Delta) \quad (4)$$

In this model, the refractive indices of the Si wafer and the SiO_2 layer are fixed to 3.882 + 0.02i and 1.457, respectively.[25] Before a PEM is prepared and investigated using ellipsometry, we determine the thickness of the native oxide layer individually for each substrate. Furthermore, the refractive index of each surrounding solution is also determined independently with a refractometer (J357 Automatic Refractometer, Rudolph, Hackettstown, NJ) at λ = 632.8 nm. Thus, the only remaining unknown sample parameters are the PEM film thickness and refractive index (d_{PEM}, n_{PEM}).

It is known that measurements at several angles of incidence allow the identification of systematic errors, as they make it impossible to fit the multiangle data with only one thickness and one index of refraction.[26] Therefore, the angle of incidence traverses during the measurement the range from 66° to 72° (with respect to the surface normal) in 1° steps (cf. Figure 2). In each position the corresponding ellipsometric angles of the sample are measured. This range was chosen because it contains the Brewster angle of a water−silica interface (71.1°) and the resulting angles Ψ and Δ are particularly sensitive to changes caused by the PEM film.

d_{PEM} and n_{PEM} are determined by a least mean square algorithm. Minimized is χ, which is defined as

$$\chi(d_{\mathrm{PEM}}, n_{\mathrm{PEM}}) = \left[\frac{1}{M}\sum_{i=1}^{M}\left(\left(1 - \frac{\Delta_i^{\mathrm{calc}}(d_{\mathrm{PEM}}, n_{\mathrm{PEM}})}{\Delta_i^{\mathrm{exp}}}\right)^2 + \left(1 - \frac{\Psi_i^{\mathrm{calc}}(d_{\mathrm{PEM}}, n_{\mathrm{PEM}})}{\Psi_i^{\mathrm{exp}}}\right)^2\right)\right]^{1/2} \quad (5)$$

Measurements are performed for M different angles of incidence. For a certain angle of incidence with index i, Δ_i^{exp} and Ψ_i^{exp} are measured and calculated (Δ_i^{calc}, Ψ_i^{calc}). In an experiment, the absolute values of Δ and Ψ can differ by an order of magnitude. Since Δ and Ψ are equally important, in eq 5 the

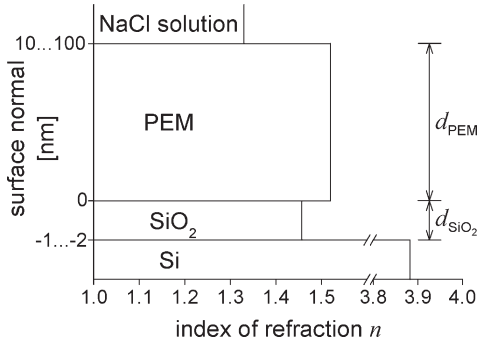

Figure 1. Scheme of refractive index profile of the sample. To quantify the measured ellipsometric angles, a slab model of the sample is used. To each slab, a constant index of refraction and thickness d are assigned. The transitions between the slabs are described as discontinuities in the refractive index profile. The PEM is represented by one of these slabs.

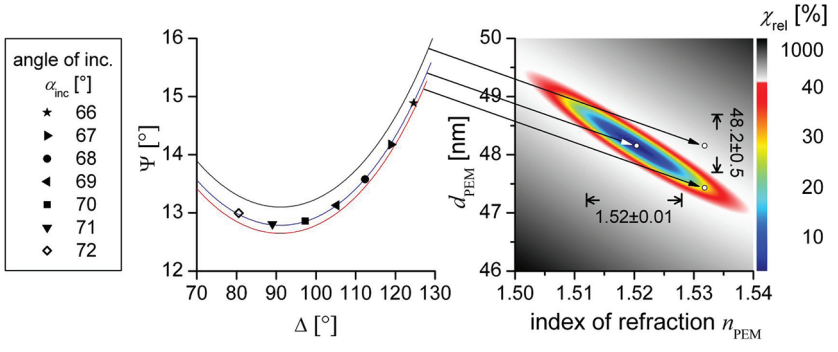

Figure 2. Ellipsometric determination of PEM thickness d_{PEM} and index of refraction n_{PEM}. (Left) Ellipsometric angles Δ and Ψ measured at different angles of incidence (black symbols) as indicated. Three exemplary $\Delta-\Psi$ trajectories (straight lines) are shown which are calculated according to eq 4 for three different pairs of d_{PEM} and n_{PEM}. (Right) Contour plot of the deviation between measured and calculated ellipsometric angles as function of d_{PEM} and n_{PEM} (calculated with eq 5). The white circles indicate the three pairs of (d_{PEM}, n_{PEM}) which lead to the straight lines shown left. χ is calculated relative to its minimum value, χ_{min} ($\chi_{\mathrm{rel}} = (\chi - \chi_{\mathrm{min}})/\chi_{\mathrm{min}}$). With χ_{rel} = 20%, one obtains n_{PEM} = 1.52 ± 0.01 and d_{PEM} = 48.2 ± 0.5 nm, as indicated.

dx.doi.org/10.1021/jp208837m |J. Phys. Chem. B 2012, 116, 1234–1243

quotients of the calculated and the measured values are considered, and not the differences between them. d_{PEM} and n_{PEM} are varied until χ reaches a minimum (cf. Figure 2).

In the case of thin films ($d < 20$ nm) the index of refraction is fixed (1.5).

EXPERIMENTAL SETUP

To perform measurements on a liquid−solid interface at several angles of incidence, the concept of Benjamins et al.[27] is implemented: special cylindrical cuvettes (Hellma, Müllheim, Germany) which work as light guides are attached to both the laser and detector arm and serve as an extension of the respective arm into the liquid environment. The end of the cuvettes which protrudes into the solution is sealed watertight with a thin plate of plane-parallel glass which was sintered by the manufacturer to the cylindrical glass tube. The light from the laser passes through the first of these windows into the liquid, is reflected at the sample, and then passes through the second window.

The cuvettes are aligned before each measurement so that their front plates are perpendicular to the laser beam. Averaging the readings of several ellipsometric zones reduces the error due to the use of windows.[28] For this reason, each measurement is carried out in both accessible ellipsometric zones.[23]

The sample cell is homemade. It consists of an elongated cutout on the top of a Teflon block (100 mm long, 43 mm wide, 32 mm high). The cell is shaped like the one described by Schmidt et al.[29] It can be filled with about 10 mL of solution. The substrate (carrying the PEM) is fixed by two Teflon brackets in a horizontal position at the bottom of the sample cell. Measurements can be performed for angles of incidence between 25 and 72° (with respect to the surface normal).

At the bottom of the Teflon block a heating element is inserted. It is connected to a thermostat (Haake F3, ThermoFisher Scientific, Karlsruhe, Germany). The temperature is controlled by an electronic thermometer (Digi-Sense Thermocouple, Cole-Parmer, Vernon Hills, IL) whose sensor is embedded into the Teflon wall next to the sample.

MULTILAYER PREPARATION BY SELF-ASSEMBLY

PEM films are prepared by sequential adsorption of oppositely charged polyelectrolytes.[2,13] Before adsorption, all deposition and washing solutions are heated to the designated deposition temperature using a thermostat (MP, Julabo GmbH, Seelbach, Germany). The cleaned substrate is horizontally aligned and fixed in the sample cell which is filled with the respective polyelectrolyte solution (30 min for each adsorption step). After each adsorption step the deposition solution is pumped out and replaced by a washing solution with the same NaCl concentration (1 min for each washing step; three replacements of the washing solution). In the last washing solution, the ellipsometric multiangle measurements are carried out. During this procedure, the PEM is never dried. It is always exposed to an aqueous solution with constant NaCl concentration and temperature.

RESULTS

Figure 3 shows null ellipsometry in situ measurements of the film growth with 1 M NaCl in the deposition and washing solutions. At 19 °C solution temperature, one observes for the first eight layers a moderate and nonlinear film growth, often described in the literature.[19] Then, the thickness increases

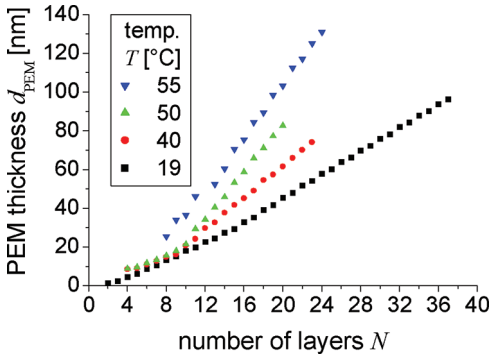

Figure 3. PSS/PAH film thickness d_{PEM} determined in situ with ellipsometry as function of number of adsorbed layers N (the aqueous solution contains 1 M NaCl; the temperature is indicated). After the adsorption of about 8−12 polyelectrolyte layers, the film grows linearly with N.

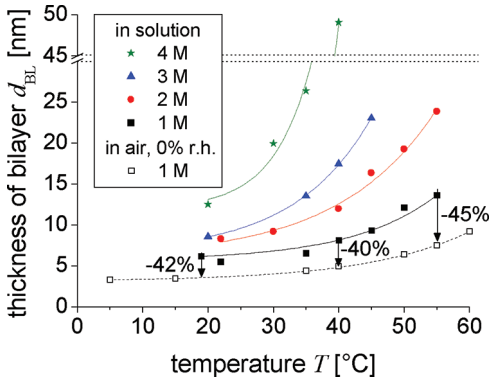

Figure 4. d_{BL}, the average thickness per PSS/PAH bilayer in the linear growth regime, as function of the preparation temperature T prepared from solutions with the indicated NaCl concentrations. Each value of d_{BL} is the average of at least 10 consecutive adsorption layers. The bilayer thickness increases both with temperature and with the salt concentration of the preparation solution. If the film is dried after preparation, the PEM thickness and thus d_{BL} decrease significantly (dry films from Gopinadhan et al.[16]).

linearly with the number of deposited layers. It has been suggested that the layers adjacent to the substrate contain more water than the linearly growing core zone of the film.

Qualitatively, the film growth is similar when the film is built at elevated temperatures. A nonlinear buildup is observed during the adsorption of the first 8−12 layers, up to 55 °C (cf. Figure 3). However, after the deposition of the first 12 layers, the film growth always turns into a linear growing scheme. Therefore, when the substrate no longer influences the film growth, d_{BL}, the thickness per deposited PAH/PSS bilayer can be determined unambiguously (cf. Figure 4). In the following, we shall focus on the linearly growing part of the film, where d_{BL} can be determined by averaging consecutive adsorption layers.

From earlier experiments it is known that the film thickness d_{PEM} increases with the temperature of the deposition solution, provided all other parameters are constant.[1,15] With in situ ellipsometry, we can monitor the thickness of a deposited polycation/polyanion bilayer in the linear growth regime. Figure 4 shows the temperature dependence of d_{BL}. For films grown at 1 M (cf. Figure 3), d_{BL} is almost constant up to preparation temperatures

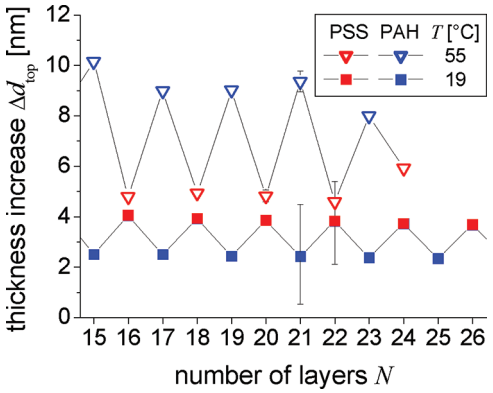

Figure 5. PEM thickness increase $\Delta d_{top} = d_{PEM}(N) - d_{PEM}(N-1)$ as function of the number of layers N (1 M NaCl aqueous solution, temperature as indicated, linear growth regime, measured with null ellipsometry). The thickness increase Δd_{top} shows an alternating pattern, depending on the number of layers. At 19 °C, an even-numbered PSS (red) layer causes a larger thickness increase than a PAH layer (blue), the so-called "odd−even" effect. At 55 °C, both the top PSS and the top PAH layer show a larger thickness than the corresponding layers at 19 °C. At 55 °C, the sequence is reversed— the odd-numbered PAH layers cause the larger thickness increase ("even−odd" effect). Also shown are four typical error bars.

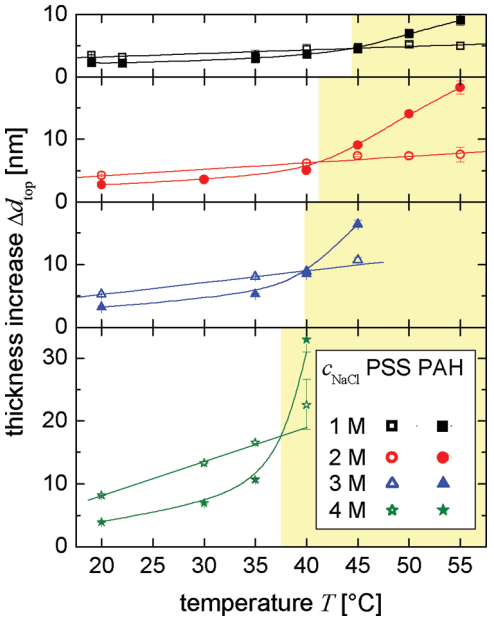

Figure 6. Average PEM thickness increase Δd_{top} due to the outermost layer for both PAH and PSS as function of preparation temperature at the NaCl concentrations indicated. Data points are obtained by averaging over at least five layers of the respective polyelectrolyte in the linear growth regime. The thickness increase due to PSS (open symbols) grows almost linearly with the preparation temperature. In contrast, the thickness increase due to PAH (full symbols) grows beyond 30−35 °C almost exponentially. The data can be grouped in two regimes: in the low-temperature regime, a PSS top layer is thicker than a PAH top layer ("odd−even" effect), whereas in the high-temperature regime, the PAH top layer is larger ("even−odd" effect, yellow area). The crossover temperature decreases with salt concentration.

of 35 °C, and then a temperature effect starts to become important and d_{BL} increases monotonously.

The films we investigate are always immersed in high salt solution. Figure 4 shows that the d_{BL} of the films immersed in 1 M NaCl solution is 40−45% thicker than the d_{BL} deduced from films prepared by the dipping technique and measured at 0% r.h.[2,16] Note that the measurements in air determine d_{BL} according to $d_{BL} = 2\, d_{PEM}/N$ (with N as the number of deposited layers). With this approach, both the layers from the precursor zone and the layers from the linearly growing part contribute. Therefore, d_{BL} as determined from the average thickness per layer pair will be always smaller than that determined from the linear growing part alone.[16] However, with the assumption that the bilayer thickness is the same as in the precursor zone and in the linear growth regime, and with different preparation techniques, a similar temperature dependence is observed. Obviously, the temperature effect is rather robust.

Furthermore, Figure 4 shows d_{BL} (from the linear growth regime) of PEMs prepared in high salt solutions containing 2, 3, and 4 M NaCl. When films made of the same number of layers (exceeding 12) are compared, d_{BL} increases monotonously with the salt concentration in solution. Furthermore, on increase of the salt concentration, the temperature dependence of d_{BL} increases. Thus, the largest value of d_{BL} (49 nm) is found at 40 °C and 4 M. Note that, even for this thick bilayer, the contour length of both polycation and polyanion exceeds d_{BL}.

Now, let us go back to the increase of the film thickness with the number of adsorbed polyelectrolyte layers (cf. Figure 3). On close inspection, one observes evidence of an odd−even effect. Considering the film prepared at 19 °C in the linear growth regime, always two consecutive layers have a similar thickness, and then a clear increase of d_{PEM} occurs. The step size $\Delta d_{top} = d_{PEM}(N) - d_{PEM}(N-1)$ is shown in Figure 5. At low temperatures, the large thickness increase occurs for the layers with an even number, that is, the polyanion layers. Obviously, each PSS layer is thicker than the previous or consecutive PAH layer, even though charge compensation occurs. This observation is in accordance with previous experiments and is called "odd−even" effect.[30]

However, when one considers the PEM thickness as function of the number of deposited layers in Figure 3, the odd−even effect cannot be discerned for preparation temperatures of 40 and 50 °C. However, at 55 °C, every second adsorbed layer contributes more strongly to the film thickness. Yet, the quantitative data analysis shown in Figure 5 demonstrates that now the odd-numbered layers are thicker than the even-numbered ones, that is, the polycation layers. Hence, at 55 °C the odd−even effect is reversed and an even−odd effect occurs.

Considering the measurements of the film growth shown in Figure 3, between 40 and 50 °C, no odd−even or even−odd effect is perceptible. To find out if an uneven film growth occurs, the average thickness Δd_{top} of the outermost PAH and PSS layers was calculated. The numbers were obtained by averaging over at least five layers of each kind in the linear growth regime. As Figure 6 demonstrates, the thickness of the top PSS increases almost linearly with the temperature. However, the thickness increase of the top PAH is more pronounced; at temperatures beyond 30−35 °C, it shows a nonlinear increase. Due to their different temperature dependencies, the thicknesses of the top polycation and polyanion layers become identical at a certain temperature. From Figure 6 one can infer that this is achieved at $T_{x\text{-over}} = 44$ °C for PEMs deposited from 1 M NaCl solution. Since at about 44 °C the top layers of polycation and polyanion have a similar thickness, it makes sense that the film thickness

depends almost linearly on the number of deposited layers at 40 and 50 °C (cf. Figure 3). Neither an odd−even nor an even−odd effect can be discerned.

For films prepared at higher salt concentrations (2, 3, or 4 M NaCl), a similar odd−even effect is observed at room temperature (cf. Figure 6). Actually, at these high ion concentrations the odd−even effect is easier to resolve by null ellispometry, since both Δd_{top} (the thickness of the top layer) and d_{BL} (the average bilayer thickness in the linear growth regime) are larger. Again, a crossover from odd−even to even−odd effect is observed. With increasing salt concentration, the crossover temperature $T_{x\text{-over}}$ decreases, from ca. 44 °C at 1 M NaCl down to 36 °C at 4 M.

With increasing salt concentration, electrostatic interactions are progressively more shielded, and therefore nonelectrostatic interactions gain in importance. This is a valid argument for both the transition temperature $T_{trans}(c_{NaCl})$ (which marks the onset of the temperature effect, i.e., the dependence of the film thickness on the deposition temperature) and the crossover temperature $T_{x\text{-over}}(c_{NaCl})$.

DISCUSSION

In this work, we investigate the growth of PEMs in dependence of salt concentration and temperature of the deposition solution. In the following, we focus only on PEM properties of samples which exhibit linear growth.

The comparison of the in situ PEM thickness (as measured with ellipsometry) with values obtained after drying (cf. Figure 4) allows to estimate a PEM water content of approximately 40%, which is in agreement with literature values.[30,31] This shows that drying of PEM samples has a prominent influence on the polymer density of the deposited layer. Moreover, recently it was shown that the temperature effect is often accompanied by a destabilization of the PEM,[1] leading to large PEM surface roughness (which obscures the application of scattering techniques to such samples). However, the films remain stable when kept in solution, and thus film characterization is possible.

The measurement of the layer thickness shows (depending on the deposition conditions) odd−even and even−odd effects. However, the ellipsometric data of Figure 5 gives evidence that the odd−even and even−odd variations observed in this work are restricted to the outmost layers of the PEM. During the recording of film growth, the thickness of the PEM triples (cf. Figure 3). If the alternation observed in PEM thickness increase Δd_{top} was a result of swelling and shrinking of the whole PEM, then Δd_{top} should increase or decrease linearly with the whole PEM thickness, yet the opposite is observed: the alternation in Δd_{top} is highly reproducible over more than 10 deposition steps deep in the linear growth regime (layers 20−30). The increase in PEM thickness is constant for odd and even layers, respectively. This observation leads to the conclusion that these odd−even and even−odd variations are limited to the outmost PEM layers.

Interestingly, Figure 6 shows that the alternation in Δd_{top} and the crossover from odd−even to even−odd behavior are general features and not restricted to 1 M NaCl. This figure can be understood as a decomposition of the bilayer thickness (which is a common quantity in experiments performed on PEMs) into the contributions of one polycation and one polyanion layer (forming one bilayer). This procedure shows that both kinds of polyions contribute differently to the increase in bilayer thickness (caused by an increase in deposition temperature): for all salt concentrations investigated and within the statistical error, a linear dependence of the temperature on the PSS layer thickness is observed. We observe with UV−vis spectroscopy a similar increase of the deposited PSS amount with increasing temperature (cf. Supporting Information, Figure S1). At room temperature, the surface coverage of a PSS layer prepared from 1 M NaCl solution is 3.5 mg/m^2. A PAH/PSS layer pair corresponds to 4.6 mg/m^2 deposited polymer. These numbers are calculated assuming that (i) the amount of positively and negatively charged monomers is identical and (ii) the PEM does not contain any monovalent counterions. On heating the 1 M NaCl solution to 55 °C, the surface coverage of one PSS layer triples.

Finally, we would like to estimate the maximum surface coverage per layer pair obtained with 4 M salt solution at 40 °C. This is done by assuming the index of refraction of the PEM is constant and independent of preparation conditions (1.51 ± 0.02). Then, the deposited polymer mass per polycation/polyanion layer pair is 37 mg/m^2.

Contrary to PSS, the top PAH layer thickness depends linearly on the temperature only for a small temperature range; then it shows a large, nonlinear increase after exceeding a certain transition temperature (30−35 °C). At the crossover temperature $T_{x\text{-over}}$, the PAH and PSS top layers exhibit the same thickness. $T_{x\text{-over}}$ decreases with increasing deposition salt concentration, which suggests that an increased electrostatic screening promotes the crossover from the odd−even to even−odd effect (this will be discussed in more detail below).

The different contributions of both polyions is an interesting behavior and probably counterintuitive at first view: theory and experiments show that most of the PEM is formed by polyions and water and that incorporated salt ions are negligible.[19] Hence, (overall) electroneutrality of the PEM can only be achieved if most of the cationic monomers are charge compensated by anionic ones, suggesting an almost 1:1 ratio of cationic and anionic monomers (intrinsic charge compensation). Therefore, one would naively expect that both polyions should show the same temperature dependence.

However, as the PEM consists of polyions and water, this simple view ignores that the layer thickness itself is no measure for the deposited amount of monomers. Hence, the 1:1 relation between the cationic and anionic monomers is only compatible to the data of Figure 6 if the water content in the PAH and PSS layers (and thus their hydration properties/their density) changes with temperature. Fortunately, several published experiments demonstrate that for PEMs with thickness above 10 nm ellipsometry is able to determine independently the PEM thickness and its index of refraction n_{PEM}.[30] Moreover, they show that the monomer density in the layers can be estimated from n_{PEM}, which allows to investigate the dependence of PEM composition on the deposition conditions.

Here, we apply this methodology to probe changes in the hydration as follows: for a given deposition condition, only ellipsometric data is used for the analysis, which belongs to PEMs with thickness exceeding 20 nm. Although this constraint ensures that PEM thickness d_{PEM} and index of refraction n_{PEM} can be determined independently by ellipsometry, n_{PEM} cannot be used directly to estimate the monomer density or level of hydration of a single deposited PAH or PSS layer, respectively. (This is obvious, as d_{PEM} and n_{PEM} refer to the whole PEM and not to the single incorporated layers.) We circumvent this problem as follows: as discussed before, the ellipsometric data of Figure 5 shows that the observed alternations are restricted to the outmost layers of the PEM; i.e., the changes in the

ellipsometric data cannot be caused by changes in the whole but only a part of the PEM. At this point, we can only speculate how many of the outmost layers contribute to the observed effect. For the sake of clarity, we will divide the PEM into two parts, i.e., the outmost/terminating layer and remaining PEM layers and estimate the refractive index n_{top} of the outmost layer indirectly by regarding the PEM properties (d_{PEM} and n_{PEM}) before and after adsorption of the last PE layer. If these PEM properties are denoted by ($d_{PEM}(N-1)$, $n_{PEM}(N-1)$) before and by ($d_{PEM}(N)$, $n_{PEM}(N)$) after the Nth adsorption step, then the refractive index n_{top} of the top layer N is calculated by

$$n_{top} = \frac{d_{PEM}(N)n_{PEM}(N) - d_{PEM}(N-1)n_{PEM}(N-1)}{\Delta d_{top}} \quad (6)$$

This formula (in which $\Delta d_{top} = d_{PEM}(N) - d_{PEM}(N-1)$ denotes the thickness of the last adsorbed layer) is based on the idea that the optical thickness of the PEM $d_{PEM}(N)n_{PEM}(N)$ can be approximated by a superposition of $d_{PEM}(N-1)n_{PEM}(N-1)$ and $\Delta d_{top}n_{top}$ (which are the optical thicknesses of all but the last of these PE layers and the terminating layer, respectively). This approximation is a linearization of the optical properties, which only leads to meaningful information if $\Delta d_{top}n_{top}$ is small compared to $d_{PEM}(N-1)n_{PEM}(N-1)$. Note that this condition is fulfilled if the top layer thickness is small compared to the remaining PEM and if the refractive indices of adjacent layers are comparable. Both requirements are fulfilled in our measurements.

Although this is a simplifying approach (the whole alternation is attributed to only one layer), the qualitative trends will not be affected by this single-layer assumption. For example, if one would perform the same calculations with the assumption that a certain number of outer layers contribute to the effects, one would only increase the denominator of eq 6 (which then contains the thickness of several layers) and hence decrease the magnitude of alternation for n_{top}. As the number of contributing layers only affects the absolute numbers but not the qualitative dependence of n_{top} (with respect to N), we will perform all calculations with the assumption that only the outmost/terminating layer contributes. This can be understood as an upper limit for changes of n_{top}.

The results of this decomposition, that is, thickness Δd_{top} and index of refraction n_{top} of the top, outmost layer in dependence on the preparation conditions are given in Figure 7. More in detail, Figure 7 (top, left and right) gives Δd_{top} and n_{top} for PEMs prepared at 19 °C (low temperature) and 55 °C (high temperature) in the presence of 1 M NaCl. At low temperatures, an odd−even effect is observed only in the thickness of the outmost layer, while the index of refraction is constant within the measurement error. Its value of approximately 1.5 and the thickness odd−even variations are quantitatively in agreement with previously performed ellipsometric studies. For example, Ruths et al.[30] studied in situ PAH/PSS multilayer formation on a lipid monolayer and report on an odd−even variation of 2 nm (PAH) and 3.5 nm (PSS) in presence of 1 M NaCl, which is in reasonable agreement with our data (2.5 and 4.2 nm, respectively). Moreover, they showed that the PAH and PSS layers are not only similar in their refractive index (around 1.47) but also in their density and thus in their water content. These findings and our work show that at (relatively) low temperatures (around 20 °C) both polyions form top layers of comparable monomer density and level of hydration.

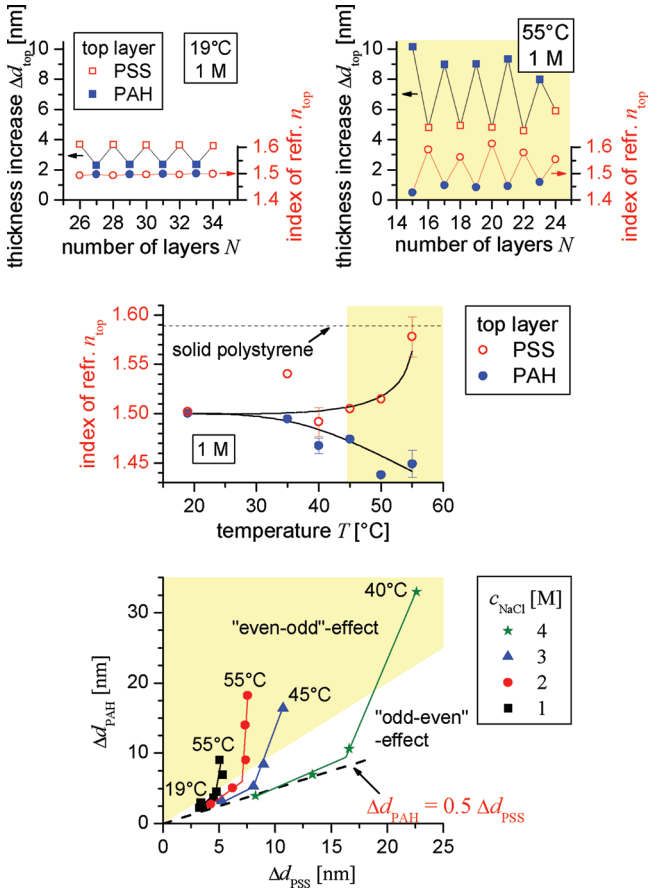

Figure 7. (Top) PEM thickness increase Δd_{top} and index of refraction n_{top} as function of the number of layers N, measured with null ellipsometry in 1 M NaCl aqueous solution, at 19 °C (left) and at 55 °C (right). For PSS as terminating layer, open red symbols are used, and full blue symbols indicate PAH. At 19 °C, when the odd-numbered top layers are thicker than the even-numbered top layers (odd−even effect), the refractive index of the top layers (calculated with eq 6) is independent of the kind of polyelectrolyte. At 55 °C, the odd−even effect is reversed. Then, also the index of refraction of the top layers oscillates, and always the even-numbered PSS layers exhibit a larger refractive index than the odd-numbered PAH layers, suggesting a pronounced hydration of the polycation. White areas indicate the odd−even effect of the film thickness increase (cf. Figure 6), yellow areas the even−odd effect. (Center) Average index of refraction n_{top} for PAH and PSS top layer as function of preparation temperature at 1 M NaCl. Data points are obtained by averaging over at least five layers of the respective polyelectrolyte in the linear growth regime. n_{top} of PAH decreases with temperature, whereas n_{top} of PSS increases. The deviation starts at 30−35 °C, a lower temperature than the crossover temperature (the latter indicates the reversal of the odd−even effect). Also shown is the refractive index of solid PSS. (Bottom) Δd_{PAH}, the average thickness per PAH top layer in the linear growth regime as function of Δd_{PSS}, the corresponding average thickness of the top PSS layer. Shown are data obtained at different temperatures and salt concentrations as indicated. The dashed line indicates $\Delta d_{PAH} = 0.5\ \Delta d_{PSS}$, an equation which is derived in consideration of the respective monomer volumes and on the assumption that the water content in the top PAH and PSS layer is the same.

However, if we now turn to samples prepared at elevated temperatures, a different picture emerges (see Figure 7, top right). Contrary to Figure 7, top left, and recent studies, alternation can be found for both the layer thickness (now with

even−odd alteration) and the index of refraction. The latter can also be resolved in the raw data, which shows that the alternation of n_{top} is not an artifact of the mathematical decomposition procedure described above (cf. Supporting Information, Figure S2). Taking the same reasoning as above, the odd−even variation of n_{top} gives clear evidence that single PAH and PSS layers differ in their water contents at elevated temperatures. In detail, for PSS a value around 1.6 is observed, which is close to its bulk value.[32] This suggests that the PSS layer is very dense and that less water is incorporated into the PSS layer with increasing deposition temperature. This decrease in level of hydration might be understood by the hydrophobic structure of PSS, which promotes secondary/nonelectrostatic interactions at higher temperatures. On the contrary, for PAH layers a refractive index around 1.45 is observed which is smaller than is value of 1.5 at approximately 20 °C. As PAH has a larger refractive index than water, this indicates a dilution of the PAH layer. Hence, an increase in deposition temperature increases the water content in the PAH layers, which is the opposite behavior compared to PSS.

Although shown for only two temperatures, this analysis is performed for all samples deposited in the presence of 1 M NaCl, and the dependence of the temperature on the refractive index of the respective polyion layers is given in Figure 7, center. Here, one observes that both polyions exhibit a similar refractive index (and thus water content) at lower temperatures (below 30−35 °C). However, on heating, the refractive index of the top PAH layer decreases and the one of the top PSS layer increases. Thus, when the deposition temperature is increased beyond 30−35 °C, the level of hydration increases monotonously for PAH and decreases monotonously for PSS. This shows that the PSS layers densify, while the PAH layers incorporate more and more water and become increasingly fluffy. This effect is obvious at 44 °C, which is also the crossover temperature for the odd−even to even−odd variations in the thickness increment. Moreover, one can infer that even−odd alterations are generally accompanied by deviations in the water content of PAH and PSS layers, respectively.

In this context, the odd−even and even−odd variations in layer thickness might be explained by a simple picture: at lower temperatures (odd−even effect) it is observed that PAH and PSS layers exhibit a similar density. Hence, as the monomer volume of PSS is almost twice that of PAH (200 Å^3 versus 97 Å^3),[1] equality in monomer density and monomer count (to ensure the 1:1 ratio of cationic and anionic monomers) is only achieved if a PSS layer is twice as thick as a PAH layer. However, an increase in temperature raises the monomer count in the PSS layers as (i) the PSS density and (ii) the PSS layer thickness increase simultaneously. Obviously, the 1:1 ratio can only be maintained if the PAH layer shows a strong, nonlinear thickness increase, which is simply a result from the combination of (i) increase in PSS monomer count and (ii) decrease in PAH density. Interestingly, the increase in PAH layer thickness is so large that the odd−even effect is inverted into an even−odd one. Moreover, this shows impressively that both polyions contribute differently to the temperature effect of the bilayer thickness.

If this view is qualitatively correct then the PSS layers should be generally twice as thick as the PAH layers, if the deposition temperature is sufficiently below the crossover to even−odd alteration. This idea is reviewed in Figure 7, bottom, which shows a $x-y$ plot of the measured PAH and PSS top layer thicknesses for all samples. Interestingly, all samples prepared below 30−35 °C give data points that are closely located to the dashed line. Note that 30−35 °C is the temperature at which the refractive indices of the different top layers no longer coincide (cf. Figure 7, center; for larger salt concentrations the data are very similar and are not shown). This shows that PSS layers are indeed twice as thick as the PAH ones if their densities or their water contents are comparable. The data points are described by this simple law for all salt concentrations investigated and for all deposition temperatures, which are sufficiently below 35 °C, when the refractive indices of the different top layers are identical. However, if the deposition temperature becomes too large, all samples show the same behavior: that is, a large rise in PAH layer thickness, which manifests itself by a steep increase and large deviations from the dashed line. Moreover, this concept shows that the classification into odd−even and even−odd is rather phenomenological (as it simply indicates which polyion contributes most to the top layer thickness), while the dashed line in Figure 7, bottom, seems to bear much more insight into the physics of the system.

To close our discussion, we want to find physical arguments why the PAH layer dilutes itself upon a temperature increase. This difference in PSS is a remarkable behavior as both polyions exhibit the same polymer backbone. Hence, one would probably expect similar secondary interactions and thus similar temperature effects of PAH and PSS, which is surprisingly not observed in the experiments. Our arguments start with the observation that the crossover temperature $T_{x\text{-over}}$ decreases with increasing deposition salt concentration. This means that the densification of the PSS layer sets in at lower temperatures, which is a clear sign that there is a balance between (repulsive) electrostatic and (attractive) nonelectrostatic interactions. At low temperatures and salt concentrations, the electrostatic interaction dominates, leading to a PSS monomer−monomer repulsion and thus a less dense PSS layer. However, with rising salt concentration, the electrostatic forces are more shielded. With rising temperature, the percentage of hydrogen bonds decreases and the balance of interactions is progressively shifted toward nonelectrostatic/secondary interactions like van der Waals forces or hydrophobicity, leading to densification of the PSS layer.

We can only speculate (motivated by the measurements) that the PAH chain does not react in a similar way on a temperature increase. For example, as the PAH monomer lacks the styrene ring it is very probable that van der Waals or hydrophobic contributions play a minor role at high temperatures (in comparison to PSS). For PSS it is known that it adsorbs onto hydrophobic surfaces and may form dense layers at high salt conditions.[33] If such an attractive contribution is missing, the polyion is unable to densify effectively.[34] This is reflected in the measurements by the observation of rather dense PSS and more diluted PAH layers at elevated temperatures. Interestingly, a fluffy chain conformation of the diluted PAH layers is in qualitative agreement with a scaling theory developed by Dobrynin et al.,[35,36] which describes the adsorption of polyelectrolyte chains onto oppositely charged surfaces in dependence of the surface charge density σ. For large σ they find the so-called "self-similar layer structure", in which both monomers and solved ions contribute to the charge (over)compensation. This leads to the formation of a rather thick but diluted PE layer above a thin dense layer at the bottom of the self-similar layer structure.

Interestingly, Dobrynin et al. show that, for the formation of this layer structure a critical surface charge density σ has to be exceeded, which depends on electrostatic (e.g., line charge density) and spatial properties (e.g., monomer size) of the

polyelectrolyte. Hence, if the (temperature induced) dilution of the PAH layers is caused by a change of the layer built up (transition to the self-similar layer structure), then the surface charge density σ of the outmost PSS layer has to exceed the critical value. This is only possible (i) if PSS changes its line charge density and/or (ii) if the monomer density increases in the PSS layer. Possibility (i) can be ruled out as PSS is known to be a strong polyelectrolyte and, thus, a change in the charging state appears to be unlikely (the pH was found to be constant ± 0.15 for all temperatures and salt concentrations). On the contrary, a temperature-induced increase in PSS density is indeed observed in the experiments. Hence, the theory of Dobrynin and co-workers might give at least a qualitative description for the dilution of the PAH layers observed in this work.

Earlier work also shows that layer deposition at elevated temperatures is accompanied by a change in layer buildup. Several publications indicate that PEMs become instable under these conditions, which is reflected by destabilization and decomposition effects of the PEM after drying. In this context, our measurements give new hints into the physics of these processes.

The deposition at lower temperatures leads to well-hydrated PE layers. Hence, PE monomers can diffuse in the PEM and form polyion complexes over several layers. This high chain interpenetration is, for example, observed in neutron reflectometry, in (Förster resonance) energy transfer measurements, and in experiments on surface forces and provides an explanation for the high stability of PEMs.[2,37] On drying, the dielectric constant changes. In water, the dielectric constant is 78 and in a dry polyelectrolyte film about 10−20.[19] As the electrostatic force is inversely proportional to the dielectric constant, the cohesive electrostatic forces between oppositely charged monomers increase on drying and stabilize the film.

In earlier experiments, we compared the outmost layer structure of PEMs in the high-temperature regime in solution and after drying.[1] We find that destabilization already starts during deposition and observe detachment of small PEM areas in tapping mode imaging in solution. Hence, it is concluded that linking between adjacent layers is reduced at elevated deposition temperatures and high salt concentrations, leading to peeling effects which are further amplified during drying of the PEM. We observed that with increasing salt concentration the destabilization temperature T_{trans} decreases (cf. Supporting Information, Table S1).

With in situ ellipsometry, we observe a similar dependence for the crossover temperature $T_{x\text{-}over}$, even though at every salt concentration the crossover temperature exceeds the destabilization temperature. Furthermore, $T_{trans}(c_{NaCl})$ shows a much more pronounced decrease with the salt concentration than the cross-over temperature $T_{x\text{-}over}(c_{NaCl})$ (from 40 °C at 1 M NaCl to 15 °C at 3 M compared to 44.3 °C down to 39.8 °C). Actually, no correlation between the density of the top layer and the stability of the PEM is found. For $T_{trans}(c_{NaCl} = 1\ M) = 40$ °C already a pronounced densification of the top PSS layer is observed. However, at $T_{trans}(c_{NaCl} = 3\ M) = 15$ °C, the thickness of the top PSS layer is twice the thickness of the top PAH layer and the densification of the PSS layer did not yet start. Therefore, layer interpenetration does not correlate with the water content and extension of the outermost polyelectrolyte layer. Apparently, the former is a property of the volume phase of the PEM while the latter describes its surface. Further insight is gained if $d_{BL}(T_{trans})$ is considered. $d_{BL}(T_{trans})$ is almost independent of T_{trans}; it amounts to 8.6 ± 0.5 nm in the respective salt solutions (cf. Figure 4 and Supporting Information, Table S1). This suggests that PAH/PSS bilayers exceeding 8.6 ± 0.5 nm are difficult to stabilize.

Summarizing, it is amazing how much the PSS density can be varied, at elevated temperatures and high salt concentration. These effects can be well understood by the densification of the PSS as observed by in situ ellipsometry in this work.

CONCLUSION

Within a liquid cell the linear growth of polyelectrolyte multilayers by LbL technique is observed with multiple angle null ellipsometry. Poly(styrenesulfonate) (PSS) and poly(allylamine hydrochloride) (PAH) are used. The salt content is varied between 1 and 4 mol/L NaCl and the deposition temperature between 20 and 55 °C. Focus of the investigations is the top layer of the PEM in the linear growth regime. Odd−even effects and even−odd effects (of thickness increase and PEM refractive index) in the dependence of the number of layers are studied. At low temperature, a top PSS layer is twice as thick as a top PAH layer (odd−even effect), consistent with the respective monomer volume and assuming the same water content for both polyelectrolyte layers, an assumption that is supported by the refractive index measurements. On heating, the thickness of a polycation/polyanion bilayer increases. Beyond 30−35 °C, the thickness of the top PAH layer grows more than the thickness of the corresponding PSS layer. Furthermore, the respective refractive indices indicate a densification of the PSS layer while the PAH layer gets more fluffy. For temperatures exceeding the crossover temperature $T_{x\text{-}over}$, a top PAH layer is thicker than a top PSS layer (even−odd effect). In earlier work it was found that beyond a critical temperature T_{trans} the films destabilize on drying; an increased roughness and a random pattern of holes is observed.[1] This critical temperature T_{trans} is below the crossover temperature $T_{x\text{-}over}$, and the temperature difference increases with the salt concentration. It is found that $d_{BL}(T_{trans})$ is 8.6 ± 0.5 nm, independent of the salt concentration. This suggests that polycation/polyanion mixing with a sufficient amount of ionic monomer−monomer bounds is only possible for a limited bilayer thickness.

ASSOCIATED CONTENT

Supporting Information. Figure S1 shows UV−vis measurements which indicate that the adsorbed amount of PSS in the PEMs in the linear growth regime rises linearly with the deposition temperature. Finally, Figure S2 compares in one exemplary measurement (c_{NaCl} = 1 M) the index of refraction of PEMs, prepared below and above the crossover temperature (≈44 °C for 1 M NaCl). Table S1 lists $T_{x\text{-}over}$, T_{trans}, and $d_{BL}(T_{trans})$ for PEMs formed at different NaCl concentrations. This material is available free of charge via the Internet at http://pubs.acs.org.

AUTHOR INFORMATION

Corresponding Author

*E-mail: helm@uni-greifswald.de (C.A.H.), block@physik.uni-greifswald.de (S.B.). Phone: +49 3834 86-4710. Fax: +49 3834 86-4712.

ACKNOWLEDGMENT

This work was supported by the BMBF (FKZ 03Z2CN11 with the ZIK HIKE project) and the Deutsche Forschungsgemeinschaft (He 1616/14-1). S.B. acknowledges support by the European Social Fund (grant no. UG 10 022) as well as the state

of Mecklenburg-Vorpommern and was supported by a fellowship of the Alfried Krupp Wissenschaftskolleg Greifswald. We thank Hubert Motschmann and Lars Dähne for helpful discussions and Laura Hippler for performing UV−vis measurements.

REFERENCES

(1) Cornelsen, M.; Helm, C. A.; Block, S. *Macromolecules* **2010**, *43*, 4300.
(2) Decher, G. *Science* **1997**, *277*, 1232.
(3) Caruso, F.; Caruso, R. A.; Möhwald, H. *Science* **1998**, *282*, 1111.
(4) Yoo, P. J.; Nam, K. T.; Qi, J. F.; Lee, S. K.; Park, J.; Belcher, A. M.; Hammond, P. T. *Nat. Mater.* **2006**, *5*, 234.
(5) Dubois, M.; Schönhoff, M.; Meister, A.; Belloni, L.; Zemb, T.; Möhwald, H. *Phys. Rev. E* **2006**, *74*, No. 051402.
(6) Hiller, J.; Mendelsohn, J. D.; Rubner, M. F. *Nat. Mater.* **2002**, *1*, 59.
(7) Goodwin, J. *Colloidal Dispersions*; Royal Society of Chemistry: London, 1982.
(8) Farrinato, R. S.; Dubin, P. *Colloid-Polymer Interactions: From Fundamentals to Practice*; John Wiley & Sons: New York, 1999.
(9) Dongen, S. v.; Stijn, F.; Hoog, H. P. M. d.; Peters, R.; Nallani, M.; Nolte, R.; Hest, J. v. *Chem. Rev.* **2009**, *109*, 6212.
(10) Dubas, S. T.; Schlenoff, J. B. *Macromolecules* **1999**, *32*, 8153.
(11) Stuart, M. A. C.; Huck, W. T. S.; Genzer, J.; Müller, M.; Ober, C.; Stamm, M.; Sukhorukov, G. B.; Szleifer, I.; Tsukruk, W.; Urban, M.; Winnik, F.; Zauscher, S.; Luzinov, I.; Minko, S. *Nat. Mater.* **2010**, *9*, 101.
(12) Sukhorukov, G. B.; Rogach, A. L.; Zebli, B.; Liedl, T.; Skirtach, A. G.; Köhler, K.; Antipov, A. A.; Gaponik, N.; Susha, A. S.; Winterhalter, M.; Parak, W. J. *Small* **2005**, *1*, 194.
(13) Decher, G.; Hong, J. D.; Schmitt, J. *Thin Solid Films* **1992**, *210/211*, 831.
(14) Klitzing, R. v. *Phys. Chem. Chem. Phys.* **2006**, *8*, 5012.
(15) Büscher, K.; Ahrens, H.; Graf, K.; Helm, C. A. *Langmuir* **2002**, *18*, 3585.
(16) Gopinadhan, M.; Ivanova, O.; Ahrens, H.; Günther, J. U.; Steitz, R.; Helm, C. A. *J. Phys. Chem. B* **2007**, *111*, 8426.
(17) Kolasińska, M.; Krastev, R.; Warszyński, P. J. *J. Colloid Interface Sci.* **2007**, *305*, 46.
(18) Ramos, J. J. I.; Stahl, S.; Richter, R. P.; Moya, S. E. *Macromolecules* **2010**, *43*, 9063.
(19) Schönhoff, M.; Ball, V.; Bausch, A. R.; Dejugnat, C.; Delorme, N.; Glinel, K.; Klitzing, R. v.; Steitz, R. *Colloids Surf., A* **2007**, *303*, 14.
(20) Köhler, K.; Shchukin, D. G.; Möhwald, H.; Suhorukov, G. B. *J. Phys. Chem. B* **2005**, *109*, 18250.
(21) Schwarz, D.; Schönhoff, M. *Langmuir* **2002**, *18*, 2964.
(22) Wong, J. E.; Diez-Pascual, A. M.; Richtering, W. *Macromolecules* **2009**, *42*, 1228.
(23) *Ellipsometry in interface science*; Motschmann, H., Teppner, R., Eds.; Elsevier: Amsterdam, 2000; Vol. 11, p 1.
(24) Azzam, R. M. A.; Bashara, N. M. *Ellipsometry and polarized light*; Elsevier: Amsterdam, 1989.
(25) *Handbook of Optical Constants of Solids*; Palik, E. D., Ed.; Elsevier: Amsterdam, 1998.
(26) Paudler, M.; Ruths, J.; Riegler, H. *Langmuir* **1992**, *8*, 184.
(27) Benjamins, J.; Jönsson, B.; Thuresson, K.; Nylander, T. *Langmuir* **2002**, *18*, 6437.
(28) Lukeš, F. *Surf. Sci.* **1969**, *16*, 74.
(29) Schmidt, S.; Motschmann, H.; Hellweg, T.; Klitzing, R. v. *Polymer* **2008**, *49*, 749.
(30) Ruths, J.; Essler, F.; Decher, G.; Riegler, H. *Langmuir* **2000**, *16*, 8871.
(31) Wong, J. E.; Rehfeldt, F.; Hänni, P.; Tanaka, M.; Klitzing, R. v. *Macromolecules* **2004**, *37*, 7285.
(32) Siqueira-Petri, D. F.; Wenz, G.; Schunk, P.; Schimmel, T.; Bruns, M.; Dichtl, M. A. *Colloid Polym. Sci.* **1999**, *277*, 673.
(33) Ahrens, H.; Förster, S.; Helm, C. A. *Phys. Rev. Lett.* **1998**, *81*, 4172.
(34) Messina, R.; Holm, C.; Kremer, K. *Langmuir* **2003**, *19*, 4473.
(35) Dobrynin, A. V.; Deshkovski, A.; Rubinstein, M. *Macromolecules* **2001**, *34*, 3421.
(36) Dobrynin, A. V.; Deshkovski, A.; Rubinstein, M. *Phys. Rev. Lett.* **2000**, *84*, 3101.
(37) Baur, J. W.; Rubner, M. F.; Reynolds, J. R.; Kim, S. *Langmuir* **1999**, *15*, 6460.